

Supplementary Information

Imaging molecular adsorption and desorption dynamics on graphene using terahertz emission spectroscopy

Y. Sano¹, I. Kawayama¹, M. Tabata², K. A. Salek¹, H. Murakami¹, M. Wang^{3,4}, R. Vajtai⁴, P. M. Ajayan⁴, J. Kono^{1,2,3,4,5}, and M. Tonouchi¹

¹Institute of Laser Engineering, Osaka University,
Yamadaoka 2-6, Suita, Osaka 565-0871, Japan

²NanoJapan Program and Department of Electrical and Computer Engineering,
Rice University, Houston, Texas 77005, USA

³Department of Electrical and Computer Engineering, Rice University,
Houston, Texas 77005, USA

⁴Department of Materials Science and NanoEngineering, Rice University,
Houston, Texas 77005, USA

⁵Department of Physics and Astronomy, Rice University, Houston, Texas 77005, USA

I. Time evolution of waveforms of terahertz radiation

Figure S1a shows the peak intensity of the terahertz (THz) wave emitted from graphene-coated InP in air as a function of time. The intensity increases with time and saturates at ~ 10 minutes. The waveform of the emitted THz wave also changes with time, as shown in Fig. S1b. After 10 minutes of excitation by femtosecond near-infrared pulses, the first peak increases and the second peak decreases (see the bottom two traces); this behavior is also seen in Fig. 1b of the main text. However, after the sample is left in air for 1 hour without laser excitation, an opposite phenomenon occurs, i.e., the first decreases and the second peak increases (the third trace from the bottom). Then further 10 minutes excitation repeats the process, i.e., the first peak increases and the second peak decreases again (the top trace). These results support our idea that the change of THz waveforms is caused by the dipoles induced by adsorbed oxygen molecules, because exposure to air promotes adsorption of molecules to graphene.

Figure S2 shows the time evolution of waveforms of THz radiation from graphene-coated InP in nitrogen (a) and dry air (b). The data was collected using the same procedure as in the case of Fig. 2 of the main text. After 10 minutes of continuous THz emission measurements (Region I), the sample was illuminated by ultraviolet UV light (365 nm) for 5 minutes (Region II), and the UV light was switched off (Region III). The results obtained in nitrogen in Fig. S2a show similar behavior to those in vacuum in Fig. 2b of the main text, and little change was observed even under UV illumination. On the other hand, the results in dry air are similar to those in oxygen in Fig. 2c of the main text, and a drastic change was observed under UV illumination. According to the mechanism we propose in this paper, the waveform changes are induced by adsorbed oxygen molecules. Therefore, dry air and oxygen gas can be considered to be the same type (both containing oxygen), whereas the nitrogen gas and dry air are free from oxygen.

II. THz radiation from graphene-coated p-type and n-type InP

We measured THz radiation from graphene-coated p-type and n-type InP, whose carrier densities at room temperature were $1.1 \times 10^{18} \text{ cm}^{-3}$ and $1.8 \times 10^{18} \text{ cm}^{-3}$, respectively, as shown in Fig. S3. Since the band bending at the surface is upward for n-type InP and

downward for p-type InP, the polarity of the emitted THz waveform switches between the two.² In addition, compared to the case of graphene-coated semi-insulating (SI-) InP, which is fully described in the main text, the intensity of emitted THz radiation is much smaller because the high free-carrier density reduces the transmittance of the THz radiation. These results agree with previous measurements.³ Furthermore, it should be noted that no significant changes in the THz waveforms can be seen over time from both p-type and n-type InP, in contrast to the case of SI-InP.

The results are explained by considering the difference of surface electric field of these three kinds of InP: n-type, p-type and SI-InP. The surface electric field, E_s , and depletion width, w , of p-type and n-type InP are expressed as follows, using Shottky's model¹:

$$E_s = \left(\frac{2eN_s\phi}{\epsilon_0\epsilon_s} \right)^{\frac{1}{2}},$$

$$w = \left(\frac{2\epsilon_0\epsilon_s\phi}{eN_s} \right)^{\frac{1}{2}},$$

where N_s is the static total carrier density and ϕ is the band-bending energy at the surface. For SI-InP, the values of E_s and w are estimated to be 9.3 kV/cm and 0.64 μm , respectively, with $\epsilon_s \sim 12.5$, $N_s \sim 10^{15} \text{ cm}^{-3}$ and $\phi \sim 0.3 \text{ eV}$ at room temperature.² On the other hand, E_s and w are estimated to be 504 kV/cm and 31.7 nm, respectively, for p-type InP, 394 kV/cm and 15.1 nm, respectively, for n-type InP using the values $\epsilon_s \sim 12.5$, $N_s \sim 1.1 \times 10^{18} \text{ cm}^{-3}$ and $\phi \sim 0.8 \text{ eV}$ for p-type, and $\epsilon_s \sim 12.5$, $N_s \sim 1.8 \times 10^{18} \text{ cm}^{-3}$ and $\phi \sim 0.3 \text{ eV}$ for n-type InP. From these calculations, it is found that surface electric fields of p-type and n-type InP are much larger than that of SI-InP. Therefore, the effect of electric dipoles induced by adsorbed oxygen molecules are expected to be much smaller for doped InP than SI-InP.

III. THz imaging with bare and graphene-coated InP

Figure S4 shows THz intensity maps for bare and graphene-coated InP. Figures S4a and S4b were obtained with the intensity of the first peak, and Figs. S4c and S4d were obtained with the intensity of the second peak in the THz waveform. It can be seen that the image contrast drastically increases once InP is coated with graphene. Moreover, it is clearly seen that the colors are inverted between Fig. S4b and S4d, which is again consistent with the fact that an increase of adsorbed molecules on graphene decreases

the intensity of the first peak and increases the intensity of second peak.

IV. Measurement with terahertz time-domain spectroscopy

Terahertz time-domain spectroscopy (THz-TDS) is a powerful tool to investigate the intraband absorption of graphene which is sensitive to Fermi level shift. Therefore, it has been used to measure changes in the optical conductivities of graphene due to the carrier doping effect of adsorbed atmospheric gases.⁴ Here we used transmission THz-TDS to measure changes due to gas desorption in the transmitted THz pulse through graphene-coated Si (100) wafer, and compared them with the data obtained by terahertz emission spectroscopy.

Figure S5a shows the transmittance of graphene-coated Si (100) in vacuum condition at various temperatures. The temperature was increased from 300 K to 420 K and the transmitted THz pulse through the sample was measured using THz-TDS. Figure S5b shows the optical conductivities of the sample in the 0.4 to 1.1 THz frequency range as a function of temperature. The optical conductivities were calculated from the Fourier-transformed spectra of the waveforms, and the average optical conductivities were normalized using the universal interband conductivity $\sigma_0 = \pi e^2/4$. A clear drop in the conductivity was observed between 360 K and 380 K, indicating that desorption of gas molecules from graphene happened in this temperature range. These data suggest that transmission THz-TDS can be used for sensing gas desorption. However, the change in the transmittance during gas desorption measured by transmission THz-TDS is less than 3% as shown in figure S5a, which means that an extremely precise measurement system is required to obtain reliable results.

On the other hand, the waveforms observed by terahertz emission spectroscopy with graphene-coated InP were drastically changed by adsorption of gases as shown in Fig. 1b in the main text. Therefore terahertz emission spectroscopy is more feasible for practical gas sensing application compared to conventional THz-TDS.

Figure Captions

Supplementary Figure S1. Time evolution of waveforms of terahertz radiation emitted from graphene-coated InP. **a**, The peak intensity of the waveforms emitted from a graphene-coated InP as a function of measurement time in air. **b**, change in the THz waveform after the samples is exposed to air for 1 hour without laser excitation.

Supplementary Figure S2. Time evolution of THz emission from graphene-coated InP in different environmental gases. **a**, dry air, **b**, nitrogen.

Supplementary Figure S3. Time-domain waveforms of terahertz radiation emitted from graphene-coated highly-doped InP. **a**, p-type InP, **b**, n-type.

Supplementary Figure S4. THz imaging with the intensity of first peak of a. bare InP and b. graphene-coated InP, and the intensity of second peak of c. bare InP and d. graphene-coated InP.

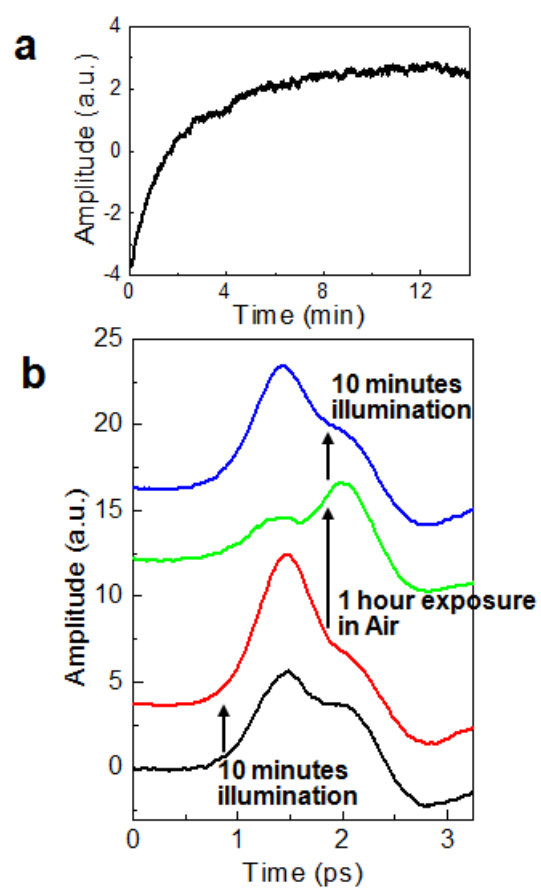
Supplementary Figure S5. Transmission THz time-domain spectroscopy with graphene-coated Si (100). **a**, Transmittance, **b**, Normalized optical conductivity.

Supplementary references

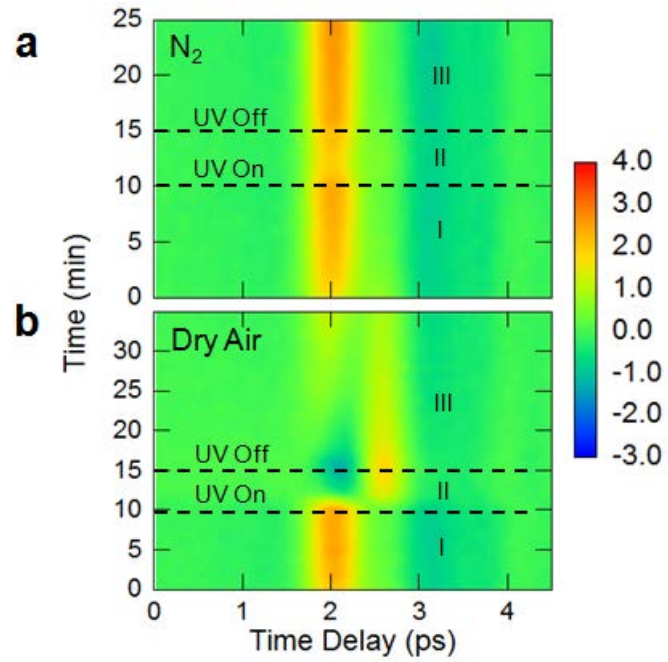
1. Sze, S. M. *Physics of Semiconductor Devices*. (Wiley, 1991).
2. Nakajima, M., Hangyo, M., Ohta, M. & Miyazaki, H. Polarity reversal of terahertz waves radiated from semi-insulating InP surfaces induced by temperature. *Phys. Rev. B* **67**, 195308 (2003).
3. Hargreaves, S. & Lewis, R. A. Single-cycle azimuthal angle dependence of terahertz radiation from (100) n -type InP. *Appl. Phys. Lett.* **93**, 242101 (2008).
4. Docherty, C. J. *et al.* Extreme sensitivity of graphene photoconductivity to environmental gases. *Nat. Commun.* **3**, 1228 (2012).

Figures

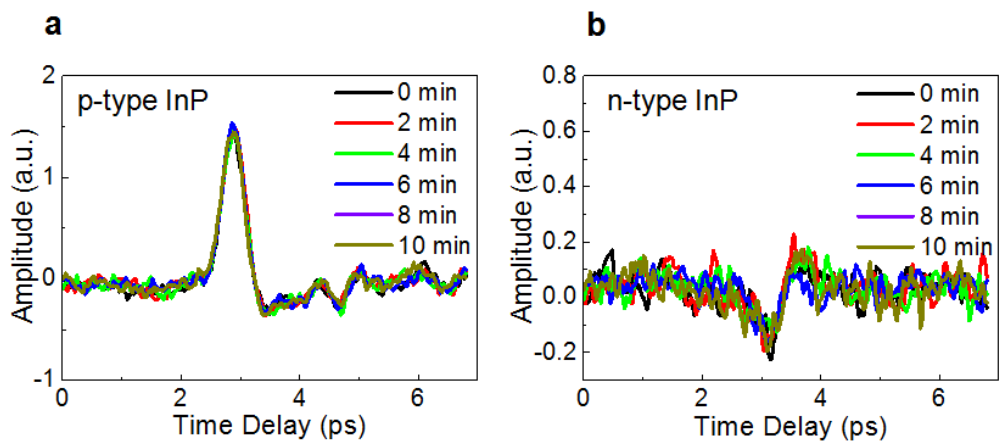
Supplementary Figure 1



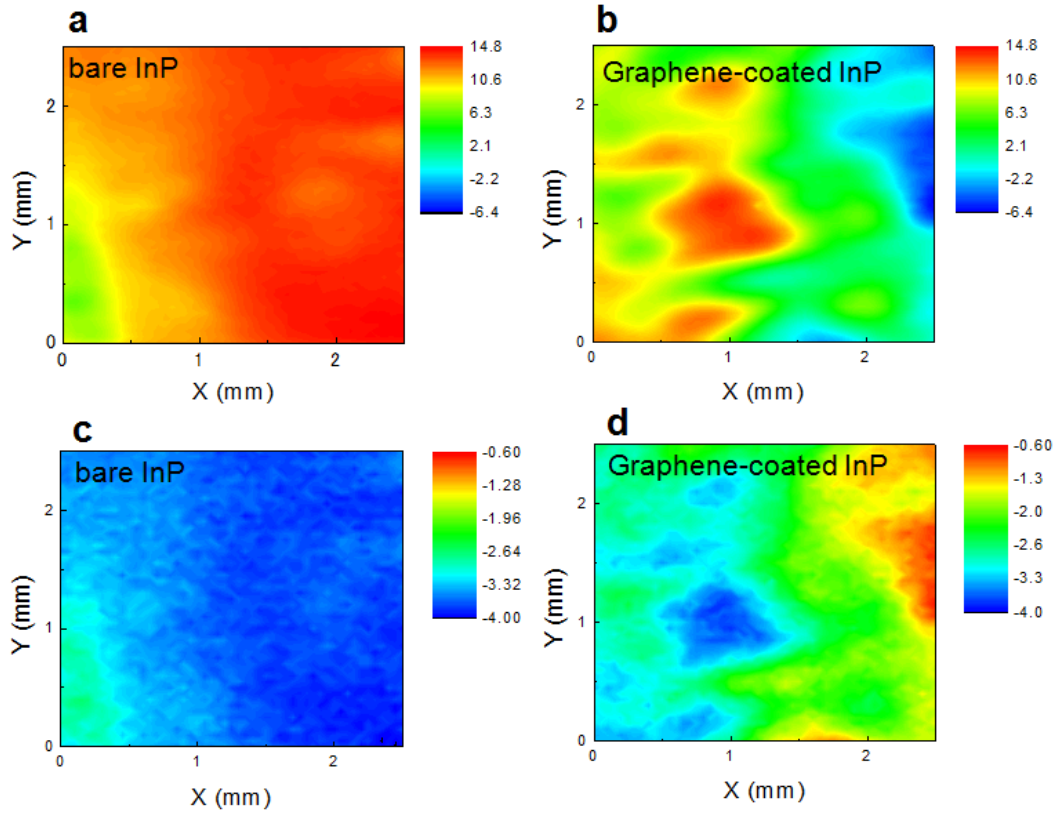
Supplementary Figure 2



Supplementary Figure 3



Supplementary Figure 4



Supplementary Figure 5

